Rare Metal Materials and Engineering
Volume 48, Issue 9, September 2019
Available online at www.rmme.ac.cn

Science Press

Cite this article as: Rare Metal Materials and Engineering, 2019, 48(9): 2779-2784.

ARTICLE

Microstructure and Properties of Soldering Sintered NdFeB Permanent Magnet to DP1180 Steel Using Zn-based Alloy

Luo Cui, Qiu Xiaoming, Ruan Ye, Lu Yuzhen, Xing Fei

Jilin University, Changchun 130025, China

Abstract: Sintered NdFeB permanent magnet (NdFeB) was firstly soldered with DP1180 steel using Zn-5Sn-2Cu-1.5Bi (ZSCB) solder. Soldering was performed in an inert atmosphere control high-frequency induction furnace, and then the microstructure, magnetic properties and shear strength were investigated by optical microscope, scanning electronic microscopy, energy dispersive X-ray analysis, NIM-2000H magnetic tester and mechanical testing machine. Results show that the interface between NdFeB/ZSCB solder forms metallurgical bonding with Nd-Fe-Zn and Fe-Zn. $FeZn_{13}$, $FeZn_{10}$ and Fe_3Zn_{10} phases form in steel side of the joints. Besides, the soldering temperature has slight influence on the magnetic properties of NdFeB. Finally, compared with adhesive bonding in traditional method, the shear strength of the soldering joints is dramatically improved by 35.38%, from 32.50 MPa to 44.00 MPa. The shear strength is high enough to cause failure in NdFeB side of the joints. Fracture of the joints is caused by large difference of thermal expansion coefficient between NdFeB and ZSCB solder as a result of high stress at the reaction layer close to NdFeB.

Key words: sintered NdFeB permanent magnet; soldering; microstructure; magnetic properties; shear strength

The sintered NdFeB permanent magnet is a kind of high-performance rare earth permanent magnetic material based on intermetallic compound $Nd_2Fe_{14}B$[1]. It has excellent magnetic properties and is widely used in many fields such as aerospace, computer technology and petrochemical industries[2-4]. Generally, the application of material is inseparable from secondary processing. The connection between sintered NdFeB permanent magnet and steel can make the best use of the magnetic properties of NdFeB, making the sintered NdFeB permanent magnet meet the requirements of modern manufacturing. However, due to its disadvantages of brittleness, poor toughness, low corrosion resistance and easy oxidation, the weldability of the sintered NdFeB permanent magnet is poor. Meanwhile, the microstructure and magnetic properties of the sintered NdFeB permanent magnet are extremely sensitive to temperature. Therefore, it is a difficult to ensure the strength of the connection without losing the magnetic properties of NdFeB. At present, the connection between NdFeB and steel is mostly achieved by means of adhesive bonding or mechanical connection[5-7]. However, adhesive bonding are brittle with poor impact resistance and low durability. Besides, mechanical connection results in increasing weight, which also will easily cause the stress concentration. Hence, it is necessary to explore a new method to achieve the high-performance connection of the sintered NdFeB permanent magnet and steel.

In recent years, with the continuous emergence of welding technology innovation, much attention have been paid to the welding technology of NdFeB. Therefore, attempts have been made to weld the sintered NdFeB permanent magnet and steel by laser spot welding. The researchers have a preliminary understanding of the weldability of sintered NdFeB permanent magnets by using laser spot welding[8-11]. However, there is a limited literature focusing on the magnetic properties of NdFeB after welding. Due to the low soldering temperature, small deformation and high quality, soldering has been widely

Received date: September 25, 2018
Foundation item: Postdoctoral Science Foundation Funded Project of China (20171M611317)
Corresponding author: Xing Fei, Ph. D., Key Laboratory of Automobile Materials of Ministry of Education, School of Materials Science and Engineering , Jilin University, Changchun 130025, P. R. China, E-mail: xingfei16@outlook.com

applied in many temperature sensitive materials, such as piezoelectric ceramic and shape memory alloys[12, 13]. Therefore, in this research, a soldering method of connecting NdFeB with steel was developed. ZSCB solder has been used for the induction-soldered NdFeB/DP1180 steel joints. The analysis is focused on microstructure, magnetic properties and shear strength of the solder joints.

1 Experiment

The based materials used in this study were the sintered NdFeB permanent magnet (N42M) and DP1180 steel. The chemical composition of NdFeB was: Nd 23.00%, Fe 73.61%, B 1.10%, Dy 1.50%, Co 0.50%, Cu 0.03%, Al 0.25%, Zr 0.01%, at%. The steel was commercially available DP1180 steel (Fe-0.146C-0.094Si-2.592Mn-0.038P-0.01S-0.662Cr-0.066Mo-0.029Al-0.018Ni, wt%). The NdFeB and DP1180 steel were machined into small blocks with dimensions of *Φ*10 mm×10 mm and 20 mm×20 mm×1.2 mm, respectively. A kind of Zn-based alloy (Zn-5Sn-2Cu-1.5Bi, wt%) was selected as the filler metal. The solidus and liquids temperatures of the filler metal measured by differential scanning calorimeter (DSC) were 386.6 ºC and 393.4 ºC, respectively.

NdFeB and DP1180 steel were polished, and then ultrasonically cleaned in acetone for 15 min. Because the Nd element in NdFeB is easily oxidized, it needs to be quickly put into SP25VIM heating furnace for soldering. The temperatures of the joints were measured by a thermocouple. When the vacuum degree was 1×10^{-1} Pa, argon was fed at a rate of 0.4 L/min. The soldering temperature was 450 ºC , and the holding time was 25 s. During the heating process, the samples were heated firstly to 400 ºC at a rate of 10 ºC /s, and then to the soldering temperature (450 ºC) at a rate of 5 ºC /s.

After soldering, the solder joints were sectioned perpendicular to the joint interface and polished through a standard method. The intergranular constituents are chemically reactive. Therefore, we polished with SiC abrasive papers up to 1200 grit and subsequently used diamond powders of 0.25 μm with a water-free lubricant[14, 15]. Optical microscopy (OM), Scanning electronic microscopy (SEM) and energy dispersive X-ray analysis (EDS) were carried out to characterize the microstructure and chemical composition of the joints and fracture surfaces. The interfacial reaction products were analyzed using X-ray diffraction (XRD). The B_r, H_{cj} and $(BH)_{max}$ are main parameters used to characterize the magnetic properties of magnetic material. In this study, those three magnetic properties of NdFeB were measured using the NIM-2000H magnetic tester. The universal testing machine (Instron 5689 Corp., USA) was used to test the shear strength at room temperature under a loading rate of 0.1 mm/min. In order to ensure the accuracy of the experiment, three samples were prepared for each test.

2 Results and Discussion

2.1 Microstructure of the solder joints

A typical microstructure of the cross-section without any voids or cracks is shown in Fig.1. A solder zone between the sintered NdFeB permanent magnet and steel, with a thickness of 251 μm, could be distinctly identified in the micrograph. On the either side of the solder zone, continuous layers of reaction products can be observed, marked as layer 1 and layer 2 in Fig.1. The EDS composition data of the locations marked "a~d" in Fig.1 are shown in Table 1. The solder zone is composed primarily of gray-based *η*-Zn (location "a"), white *ε*-$CuZn_5$ (location "b"), dark gray *β*-Sn (location "c") and white precipitate Bi (location "d") located at grain boundaries of *β*-Sn. The observation is consistent with the previous studies by F. Xing[16].

A 0.65 μm thin continuous layer of reaction product, marked "1" in Fig.2a, formed all along the sintered NdFeB permanent magnet. The EDS maps of various elements are shown in Fig. 2b~2e. It can be seen that a small amount of $Nd_2Fe_{14}B$ phase was stripped from the base metal into the soldering seam. The chemical composition across the reaction layer 1 is shown in Fig.2f. The lining analysis shows that the interface consists of two layers, "1a" and "1b". In order to estimate the chemical composition of these two layers, spot scanning analysis was carried out (Table 2). According to the result, the layers of Nd-Fe-Zn and Zn-Fe compounds were formed. The formation of Nd-Fe-Zn ternary system ($NdFe_{5.5}Zn$ and $NdFe_{1.5}Zn_{5.5}$ are the two possible phase) when Zn diffusion induced precipitation along grain boundaries in Zn-coated NdFeB magnets was initially characterized by Y. Hu[17]. The Zn atoms in the solder diffused along the grain boundary, replacing the Fe atoms in the $Nd_2Fe_{14}B$ phase to form the Nd-Fe-Zn ternary phase. Then, the substituted Fe atoms transferred to the grain boundary and combined with the Zn atoms at the grain boundaries to generate Fe-Zn binary phase.

The OM micrograph of the DP1180 steel-ZSCB solder interface in Fig.3a shows that a 17.8 μm thickness reaction layer

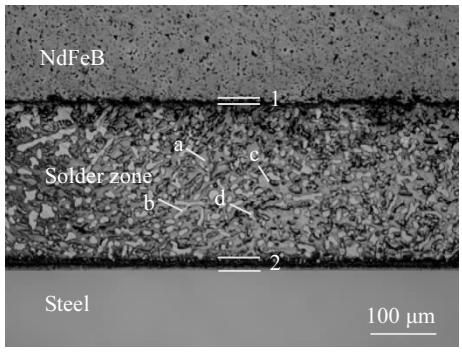

Fig.1 OM micrograph showing the microstructure of the cross-section of a joint between sintered NdFeB permanent magnet and steel using ZSCB solder at 450 ℃ for 25 s

Table 1 Chemical composition of locations marked in Fig.1 (wt%)

Region	Composition				Potential phase
	Zn	Sn	Cu	Bi	
a	98.43	0.24	1.33	-	η-Zn
b	84.32	-	15.68	-	ε-$CuZn_5$
c	-	95.41	-	4.59	β-Sn
d	-	3.22	-	96.78	Bi

has formed uniformly throughout this interface. The reaction zone at this interface consists of three layers, marked as "2a" , "2b" and "2c". Therefore, in order to know the elemental composition of layer, the reaction layer was subjected to spot scanning analysis. The composition of the reaction layer 2a was: Zn 89.80 at%, Sn 0.90 at%, Cu 2.29 at%, Bi 0.05 at% and Fe 6.96 at%. While, the composition of the reaction layer 2b was: Zn 85.11 at%, Sn 0.27 at%, Cu 0.93 at% and Fe 13.69 at%. The composition of the reaction layer 2c was: Zn 74.32 at%, Sn 0.13 at%, Fe 25.55 at%. In order to more clearly investigate the phase along steel, XRD was conducted. The results of XRD analysis are shown in Fig. 3b. The peaks of the η-Zn, β-Sn, Bi and $CuZn_5$ phases presenting in the solder alloy, along with those of α-Fe from the substrate, were detected in the profiles. The presence of $FeZn_{13}$ and $FeZn_{10}$ convincingly indicates their formation at the DP1180 steel-ZSCB solder interface. The content of the Fe_3Zn_{10} phase is too small, so XRD cannot detect it. The sequential nucleation of the Fe-Zn phase layer occurs at the interface beginning with the $FeZn_{13}$ phase layer, followed by the $FeZn_{10}$ phase layer[18]. The formation of $FeZn_{13}$, $FeZn_{10}$ and Fe_3Zn_{10} can be explained according to the binary phase diagram of Fe-Zn. Zn atoms diffused into the DP1180 dual phase steel and reaction could be described as follow: $Fe_{(s)} + Zn_{(l)} \rightarrow FeZn_{13} + FeZn_{10} + Fe_3Zn_{10}$[19].

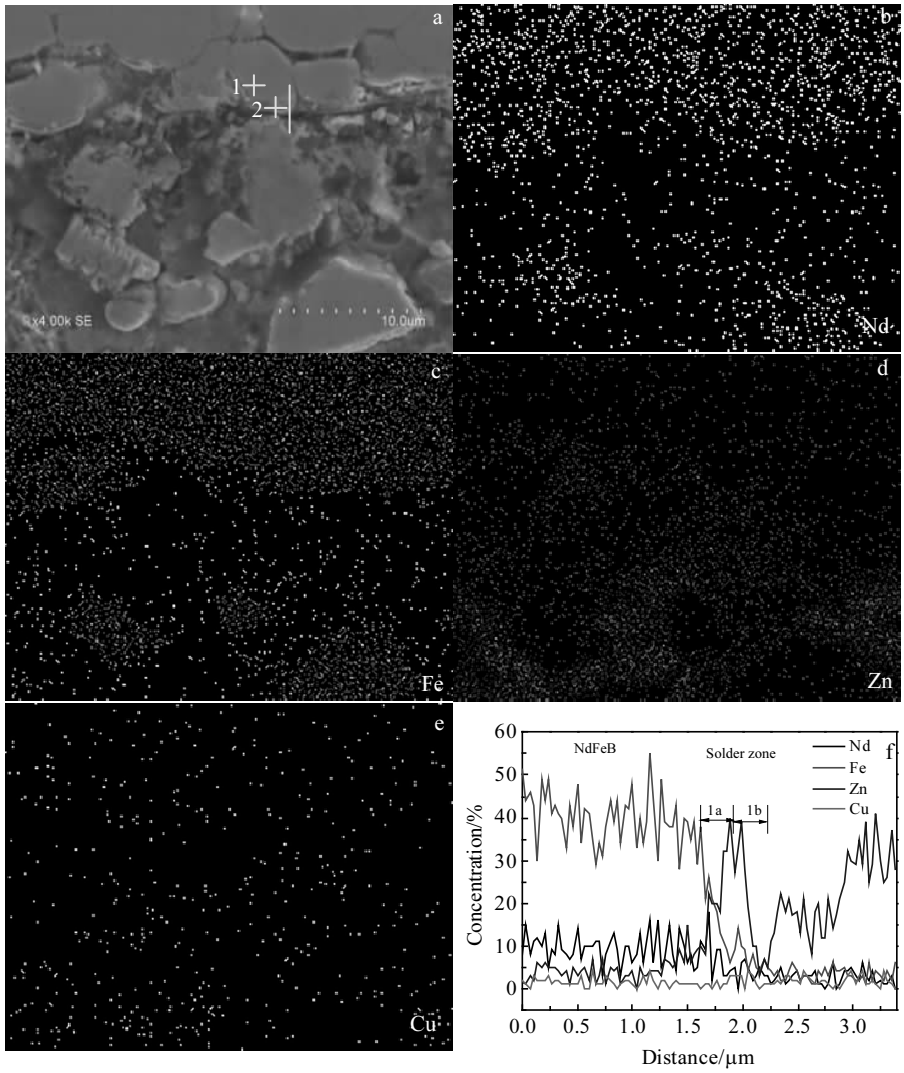

Fig.2 SEM micrograph closing to NdFeB (a) and EDS maps of Nd (b), Fe (c), Zn (d), Cn (e), EDS lining analysis across the NdFeB-ZSCB solder interface of the solder joints (f)

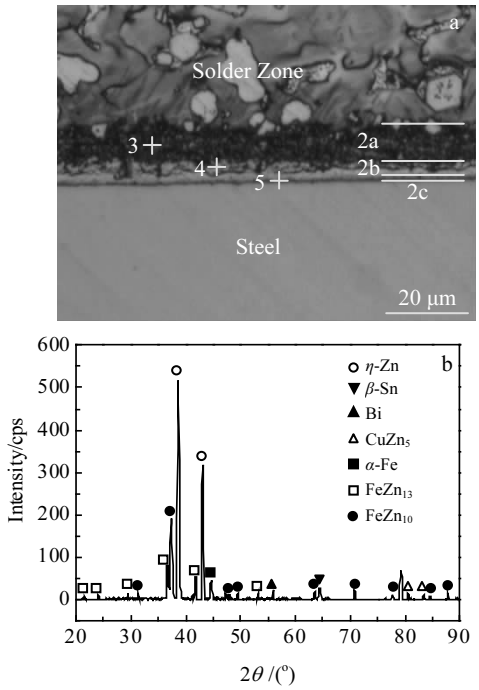

Fig.3 OM micrograph close to DP1180 steel (a) and X-ray diffraction pattern from DP1180 steel, reacted with ZSCB solder at 450 ℃ for 25 s (b)

Table 2 Chemical composition of locations marked in Fig.2 and Fig.3 (wt%)

Region	Composition						Potential phase
	Zn	Sn	Cu	Bi	Nd	Fe	
1	9.79	0.31	0.33	0.06	9.71	79.80	Nd-Fe-Zn
2	91.59	0.69	0.84	-	0.32	6.56	Fe-Zn
3	89.80	0.90	2.29	0.05	-	6.96	$FeZn_{13}$
4	85.11	0.27	0.93	-	-	13.69	$FeZn_{10}$
5	74.32	0.13	-	-	-	25.55	Fe_3Zn_{10}

2.2 Effect of soldering on magnetic properties

Sintered NdFeB permanent magnets are functional materials whose magnetic properties are extremely sensitive to the change of temperature. After soldering, it is necessary to ensure that the magnetic properties of NdFeB do not decrease dramatically.

The comparison of the microstructure of the sintered NdFeB permanent magnet before and after soldering are shown in Fig.4. It can be seen that the main magnetic phase ($Nd_2Fe_{14}B$) of the magnet is gray and distributed nonuniformly. The black parts are the Nd-rich phase existing along grain boundaries or at intersections of grain boundaries of the main phase[20]. The areal fraction of metallic neodymium in the sintered NdFeB permanent magnet is 10.71%. In the case of soldering, the areal fraction of metallic neodymium slightly decreases to 10.06%. Compared with the grains of matrix phase of the magnet before soldering, the grains after soldering are coarser. And the average grain size of the NdFeB increases from 6.97 μm to 7.08 μm. Grain morphology and size of the sintered NdFeB permanent magnet material have not been significantly changed before and after soldering. Fig.5 is the demagnetization curves of NdFeB before and after soldering. The B_r, H_{cj} and $(BH)_{max}$ of NdFeB after soldering range from 1.314 to 1.292 T, 1257.3 kA/m to 1203.2 kA/m and 329.2 kJ/m^3 to 311.0 kJ/m^3, slightly decreased by 1.67%, 4.30% and 5.54%, respectively.

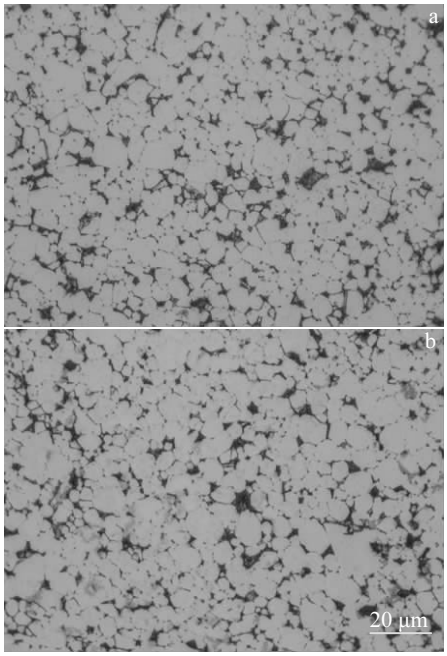

Fig.4 Microstructure of the sintered NdFeB permanent magnet before (a) and after (b) soldering

The magnetic properties of NdFeB are extremely sensitive to their microstructure, especially a thin continuous Nd-rich layer surrounding the $Nd_2Fe_{14}B$ grains and the grain size of $Nd_2Fe_{14}B$[21, 22]. With the grain size increasing, the magnetostatic interaction increases, resulting in a decrease in magnetic properties[23]. According to the result, the soldering temperature has little influence on the magnetic properties of sintered NdFeB permanent magnets.

2.3 Mechanical property of the joints

Fig.6 is stress-strain curves of solder joints and adhesive bonding. As shown in Fig.6, the shear strength and elongation of solder joints were at the average of 44.00 MPa and 0.24%, respectively. While, the mechanical properties of adhesive bonding were 32.50 MPa for shear strength and 0.04% for elongation. Compared with adhesive bonding, the shear strength and elongation of solder joints increased by 35.38% and 500.00%, respectively.

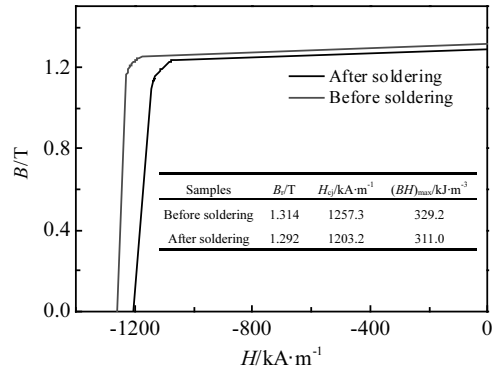

Samples	B_r/T	H_{cj}/kA·m^{-1}	$(BH)_{max}$/kJ·m^{-3}
Before soldering	1.314	1257.3	329.2
After soldering	1.292	1203.2	311.0

Fig.5 Demagnetization curves of NdFeB before and after soldering

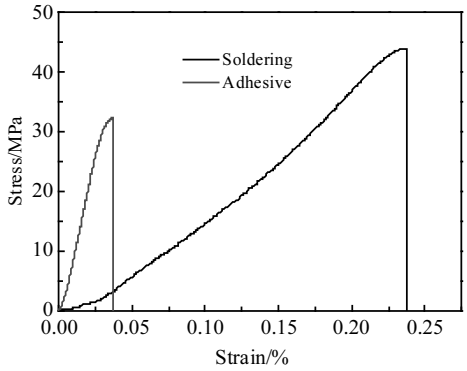

Fig.6 Stress-strain curves of the solder joints

Fig. 7a is morphology of fracture surface. The fracture was ice-sugar-like, which was the same as the fractures of NdFeB. In order to further determine the location of the fracture, the fracture was subjected to EDS analysis, and the analysis results are shown in Fig. 7b. EDS shows the presence of peaks of Zn and Cu of the solder. Therefore, it could be concluded that fracture occurs at reaction layer close to NdFeB. During the heating and cooling process, the difference of physical and chemical properties between NdFeB and ZSCB solder leads to residual stress at the interface, reducing the bonding strength of NdFeB/ZSCB solder. Thermal residual stresses σ^{th} in the NdFeB arising from the different thermal expansion coefficients between NdFeB and ZSCB solder can be calculated according to Eq.(1), where E is the Young's modulus, $\Delta\alpha$ represents the mismatch in the thermal expansion coefficients between NdFeB and filler alloy and ΔT is the temperature difference between the soldering temperature and room temperature.

$$\sigma^{th} = E \cdot \Delta\alpha \cdot \Delta T \quad (1)$$

Assuming a soldering temperature of 723 K and using the corresponding values for NdFeB and ZSCB solder (E_{NdFeB}= 1.5×10^5 MPa[24], $\Delta\alpha$=34.5×10^{-6} K^{-1}[25, 26], ΔT=430 K), thermal residual stress is as high as 2225.25 MPa. Therefore, it is easy to lead to stress concentration, which results in the failure at interface along NdFeB.

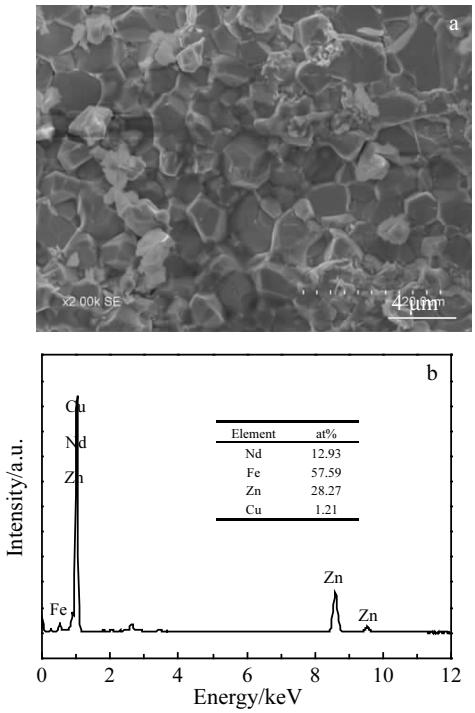

Element	at%
Nd	12.93
Fe	57.59
Zn	28.27
Cu	1.21

Fig.7 Morphology (a) and EDS analysis (b) of fracture surface

3 Conclusions

1) When the soldering temperature is 450 ℃ and the holding time is 25 s, on the side of the sintered NdFeB permanent magnet, the reaction layer appears, which mainly consists of Nd-Fe-Zn ternary phase and Fe-Zn binary phase. Three Fe-Zn compound layers, $FeZn_{13}$, $FeZn_{10}$ and Fe_3Zn_{10}, are observed to border steel substrate.

2) The B_r, H_{cj} and $(BH)_{max}$ of NdFeB after soldering slightly are decreased by 1.67%, 4.30% and 5.54%, respectively.

3) Compared with adhesive bonding, the mechanical properties of the solder joints show significantly improvement in strength and elongation (44 MPa and 0.24%), with the increase of 35.38% and 500.00%, respectively.

4) The solder joints are fractured at the interface adjacent to NdFeB due to the thermal residual stresses with the maximum shear strength of 44.0 MPa.

References

1 Wang Y L, Zhang G Q, Huang Y L *et al*. *Rare Metal Materials and Engineering*[J], 2018, 47(1): 146 (in Chinese)

2 Gutfleisch O, Willard M A, Brück E *et al*. *Advanced Materials*[J], 2011, 23(7): 821

3 Matsuura Y. *Journal of Magnetism and Magnetic Materials*[J],

2006, 303(2): 344
4 Fabiano F, Calabrese L, Capri A *et al*. *Science of Advanced Materials*[J], 2017, 9(7): 1141
5 Zhou J T. *Micromotors*[J], 2015, 48(3): 100
6 Hyo J K, Dong H K, Chang S K *et al*. *IEEE Transactions on Magnetics*[J], 2007, 43(6): 2522
7 Sang-Soo J, Fernando R, Rodolfo E D *et al*. *IEEE Transactions on Biomedical Circuits and Systems*[J], 2009, 3(5): 348
8 Chang B H, Bai S J, Li X G *et al*. *Journal of Tsinghua University, Science and Technology*[J], 2008, 48(11): 1904
9 Chang B H, Bai S J, Du D *et al*. *Journal of Materials Processing Technology*[J], 2010, 210(6): 885
10 Chang B H, Yi C H, Du D *et al*. *Journal of Tsinghua University (Science and Technology)*[J], 2014, 54(9): 1138
11 Chang B H, Du D, Yi C H *et al*. *Metals*[J], 2016, 202(6): 1
12 Bucur R A, Badea L, Bucur A L *et al*. *Journal of Alloys and Compounds*[J], 2015, 630: 43
13 Tillmann W, Momeni S. *Sensors and Actuators A: Physical*[J], 2015, 221: 9
14 Witold S. *Journal of Magnetism Magnetic Materials*[J], 2006, 301(2): 546
15 Folks L, Woodward R C. *Journal of Magnetism Magnetic Materials*[J], 1998, 190(1): 28
16 Xing F, Yao J, Liang J W *et al*. *Journal of Alloys and Compounds*[J], 2015, 649: 1053
17 Hu Y, Jones I P, Aindow M *et al*. *Journal of Magnetism and Magnetic Materials*[J], 2003, 261(1): 13
18 Marder A R. *Progress in Materials Science*[J], 2000, 45(3): 191
19 Jordan C E, Marder A R. *Journal of Materials Science*[J], 1997, 32(21): 5593
20 Sasaki T T, Ohkubo T, Une Y *et al*. *Acta Materialia*[J], 2015, 84: 506
21 Kronmüller H, Schrefl T. *Journal of Magnetism and Magnetic Materials*[J], 1994, 129(1): 66
22 Hono K, Sepehri-Amin H. *Scripta Materialia*[J], 2012, 67: 530
23 Woodcock T G, Zhang Y, Hrkac G *et al*. *Scripta Materialia*[J], 2012, 67(6): 536
24 Li A H, Dong S Z, Li W. *Metallic Functional Materials*[J], 2002, 9(4): 7
25 Smithells C J, Gale W F, Totemeier T C. *Smithells Metals Reference Book*[M]. Oxford: Kidlington, 2003
26 Hanitsch R. *Rare-Earth Iron Permanent Magnet*[M]. Oxford: Clarendon Press, 1996

Zn 基钎料钎焊烧结 NdFeB 与 DP1180 钢接头微观组织及性能

罗　萃，邱小明，阮　野，卢裕臻，邢　飞
(吉林大学，吉林 长春 130025)

摘　要：采用 Zn-5Sn-2Cu-1.5Bi（ZSCB）钎料实现了烧结 NdFeB 永磁材料（NdFeB）与 DP1180 钢的钎焊连接。在惰性气氛控制的高频感应炉中进行钎焊，采用 OM、SEM、EDS、微区 XRD 和 NIM-2000H 磁性测试仪等手段分析了接头界面的微观组织结构、NdFeB 的磁性能和接头剪切强度。结果表明，NdFeB 与 ZSCB 钎料形成 Nd-Fe-Zn 和 Fe-Zn 冶金结合，$FeZn_{13}$、$FeZn_{10}$ 和 Fe_3Zn_{10} 相在 DP1180 钢侧的界面处形成。焊接温度对 NdFeB 的磁性能影响较小。与传统方法的粘接相比，接头的抗剪切强度从 32.50 MPa 提高到 44.00 MPa，提高了 35.38%。由于 NdFeB 和 ZSCB 钎料之间的热膨胀系数差异很大，在接近 NdFeB 的反应层处产生较高的残余应力，导致接头从 NdFeB 界面处断裂。

关键词：烧结NdFeB永磁材料；软钎焊；微观组织；磁性能；剪切强度

作者简介：罗 萃，女，1994 年生，博士生，吉林大学材料科学与工程学院，吉林 长春 130025，E-mail: luocui16@mails.jlu.edu.cn